II CONGRESSO NACIONAL DE ENGENHARIA MECÂNICA
II NATIONAL CONGRESS OF MECHANICAL ENGINEERING
12 a 16 de Agosto de 2002 - João Pessoa – PB

INERT AND IDEAL SIMULATIONS OVER A RE-ENTRY VEHICLE

Carlos Alberto Rocha Pimentel
Universidade do Vale do Paraíba – UNIVAP
São José dos Campos - SP 12244-000 – BRAZIL
cearapim@univap.br

Heidi Korzenowski
Universidade do Vale do Paraíba – UNIVAP
São José dos Campos - SP 12244-000 – BRAZIL
heidi@univap.br

Abstract. *The present work performs inviscid and viscous hypersonic flow simulations over a re-entry body. A small ballistic re-entry vehicle SARA configuration is numerically investigated by using the Euler and the full Navier-Stokes equations. In the inviscid formulation one considers inert gas flow, and in the viscous case one considers ideal gas flow simulations. The governing equations are discretized in conservative form in a cell centered, finite volume procedure for unstructured triangular grids. Spatial discretization considers upwind scheme. A MUSCL reconstruction of primitive variables is used in order to determine left and right states at interfaces. Time march uses, an explicit 2nd-order accurate, 5-stage Runge-Kutta time stepping scheme. 79% of Nitrogen and 21% of Oxygen composes the inert gas. Freestream Mach 9 and 10 flows were selected to conduct numerical investigations.*

Keywords: *hypersonic flow simulation, finite volume, unstructured grid*.

1. INTRODUCTION

The development of efficient numerical solvers is very important owing to the difficulties and high costs associated with the experimental work at high speed flows. The hypersonic fluid flow simulation over a blunt-nosed body is characterized by a strong detached shock ahead the body. This phenomenon is particularly interesting because the curved bow shock is a normal shock wave in the nose region, and away from this, one has all possible oblique shock solutions for a given freestream Mach number (Anderson, 1989).

A finite volume formulation of compressible Euler and Navier-Stokes equations in conservative form has been considered. A high-resolution scheme is employed in order to obtain a good spatially resolution of the flow features. Many numerical upwind methods have been derived. In this work the simulations are performed by using a flux-vector splitting scheme (van Leer, 1995). The second-order scheme considers a MUSCL approach (Hirsh, 1990), that is, the interface fluxes are formed using left and right states at the interface, which are linearly reconstructed by primitive variable extrapolation on each side of the interface. The Euler and Navier-Stokes equations are discretized in a cell centered based finite volume procedure on triangular meshes. Time march uses an explicit, 2^{nd}-order accurate, five-stage Runge-Kutta time stepping scheme (Mavriplis, 1988).

The hypersonic flow simulations are performed over a blunt-nosed body. The freestream Mach number M_∞=9 and M_∞=10 was select to conduct the numerical investigations. Results indicate that the scheme could adequately capture the flowfield features.

2. MATHEMATICAL MODEL FOR A NUMERICAL SOLUTIONS

The two-dimensional time-dependent, compressible Navier-Stokes equation may be described, in conservative vector form, by

$$\frac{\partial Q}{\partial t}+\frac{\partial E}{\partial x}+\frac{\partial F}{\partial y}=0 \tag{1}$$

where E and F are conservative flux vectors, and can be expressed as the sum $E=E_e+E_v$ e $F=F_e+F_v$, respectively. Q is the vector of conservative quantities. If the equations are discretized in a cell centered finite volume procedure, the discrete vector of conserved variables, Q_i, is defined as na average over the *i_th* control volume. In this context, the flow variables can be assumed as attributed to the cetroid of each cell (Korzenowski, 1998). The equation (1) can be written in integral form for the *i_th* control volume as

$$\frac{\partial}{\partial t}(V_i Q_i)+\int_S[(E_e-E_v)dy-(F_e-F_v)dx]=0 \tag{2}$$

where V represents the area of the control volume and S its boundary.

The inert flow will be computed using the unsteady 2-D Navier-Stokes equations, thus neglecting viscous terms and molecular transport. In this case, the vector of conservative variables, Q, and E, F flux vectors are defined as (Pimentel, 2000)

$$Q=[\rho,\rho u,\rho v,\rho\varepsilon,\rho Y_{N2},\rho Y_{O2}],\qquad E=\begin{bmatrix}\rho u\\ \rho u^2+p\\ \rho uv\\ \rho Y_{N2}u\\ \rho Y_{O2}u\end{bmatrix},\quad F=\begin{bmatrix}\rho v\\ \rho v^2+p\\ v(\rho\varepsilon+p)\\ \rho Y_{N2}v\\ \rho Y_{O2}v\end{bmatrix} \tag{3}$$

with p, Y_K and ε given by

$$Y_K=1-\sum_{k=1}^{K-1}Y_k\ ,\qquad p=\rho RT\sum_{k=1}^{K}\frac{Y_K}{W_K},\qquad \varepsilon=\sum_{k=1}^{K}Y_k e_k+\frac{1}{2}\left(u^2+v^2\right) \tag{4}$$

where

$$e_k=h_k^0+\int_{T_0}^{T}c_{pk}dT-\frac{p}{\rho} \tag{5}$$

In these equations ε is the total energy per unit of mass, *e* is the internal energy, *R* is the universal gas constant. The internal energy, the standard-state enthaply and the specific heat at constant pressure per unit of mass of species *k* are noted e_k, h_k^0 and c_{pk}. Y_k and W_k are the mass fraction and the molecular weight of chemical species *k*, respectively.

3. SPATIAL DISCRETIZATION ALGORITHM

The numerical approach discretized the Euler and Navier-Stokes equations in conservative form in an upwind, finite volume context considering an unstructured grid made up of triangles. For the flux-vector splitting case, a van Leer formulation has been tested. The 2nd-order flux-vector splitting scheme has used a MUSCL-type extrapolation (Hirsh, 1967) in order to determine left and right states at the interfaces. A minmod limiter was used in order to avoid oscillations. Time integration used an explicit, 2nd-order accurate, hybrid method, which evolved from the consideration of Runge-Kutta time stepping scheme.

The convective operator, $C(Q_i)$, which discretize the surface integral of equation (2), is defined for the van Leer flux vector splitting scheme by the expression

$$C(Q_i) = \sum_{k=1}^{3} (E_{ik}\Delta y_{ik} - F_{ik}\Delta x_{ik}) . \tag{6}$$

The interface fluxes, E_{ik} and F_{ik} are defined as

$$E_{ik} = E^{+}(Q^{-}) + E^{-}(Q^{+}), \quad F_{ik} = F^{+}(Q^{-}) + F^{-}(Q^{+}) \tag{7}$$

where Q_L and Q_R are the left and right states at the *ik* interface obtained by linear extrapolation process.

4. NUMERICAL RESULTS

The small ballistic re-entry vehicle SARA configuration was used to perform the numerical simulations. Results obtained for a viscous flow over this hypersonic body at Mach number 10 are presented. The mesh used for the viscous flow simulations consists of 22044 nodes and 43376 volumes. This mesh was generated with 16 layers in the near wall viscous region. On the rest of the computational domain an unstructured mesh was generated. The mesh and a detail near the surface are presented in Figure 1.

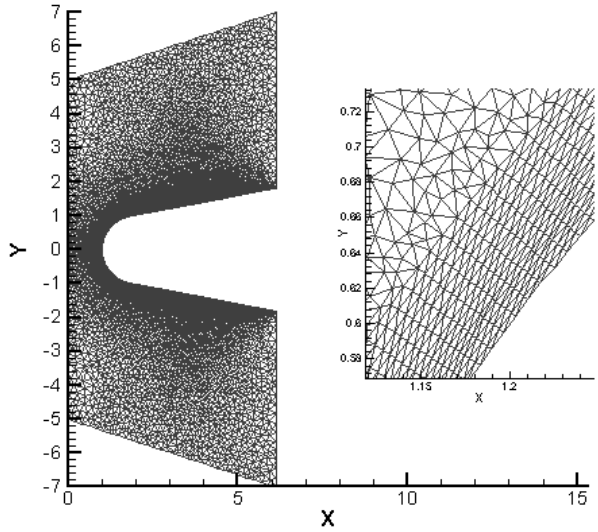

Figure 1. Mesh used for viscous flow simulations, freestream Mach number 10.

The Mach number contours, obtained considering Mach number 10, Reynolds number 100.000 and Prandtl number 0.72 are presented in Figure 2.

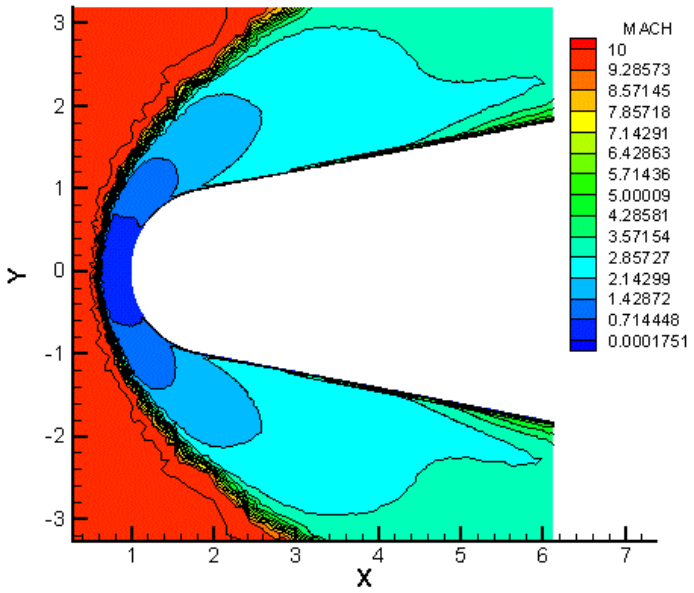

Figure 2. Mach number contours obtained with the viscous flow simulation.

The Mach number contours obtained with the second-order Liou scheme are presented in Figure 2. The contours indicate that the flow features are well captured by this solution, the bow shock and the flow expansion over the body are well represented. One can see that at the nose of the body the shock is normal, and away from this the shock wave gradually becomes curved and weaker. The hypersonic flow ahead the shock becomes subsonic behind this one, that is, there is a strong compression of the flow in this region. Slightly above the nose region, the shock is oblique and pertains to the strong shock-wave solution. As we move further along the shock, the wave angle becomes more oblique, and the flow deflection decreases until reach the maximum deflection angle. From the nose region until this point the flow is subsonic. Above this one, all points on the shock correspond to the weak shock solution. This region is characterized by supersonic flow. The temperature contours are presented in Figure 3.

The oscillations presented in the strong shock ahead the body, observed in Mach and temperature contours, can be improvement by use of a more refined mesh. However, one has some difficulties to use the refinement procedure in sense that the sensor, used to construct the adaptive mesh, was not appropriate to viscous case. A new sensor definition must be done.

The pressure distribution over the surface, considering the viscous case is presented in the Figure 4. On can see that the mesh in the viscous region was adequately refined, in sense that no oscillations appear in the pressure distribution. In the viscous case, all properties are dimensionless.

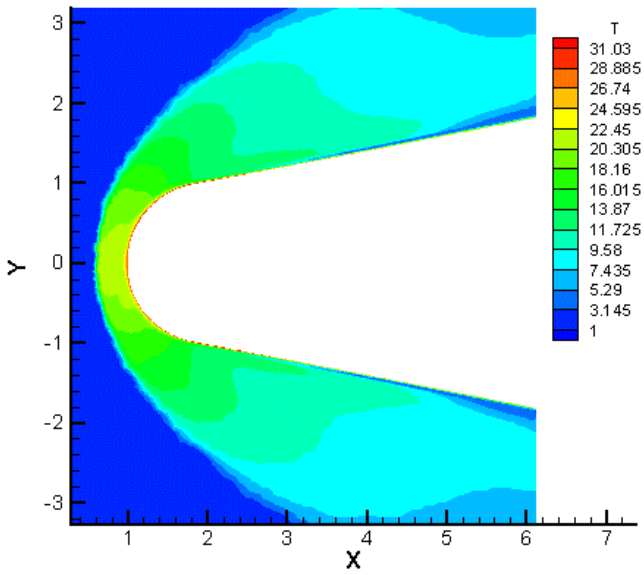

Figure 3. Temperature contours obtained with the viscous simulation.

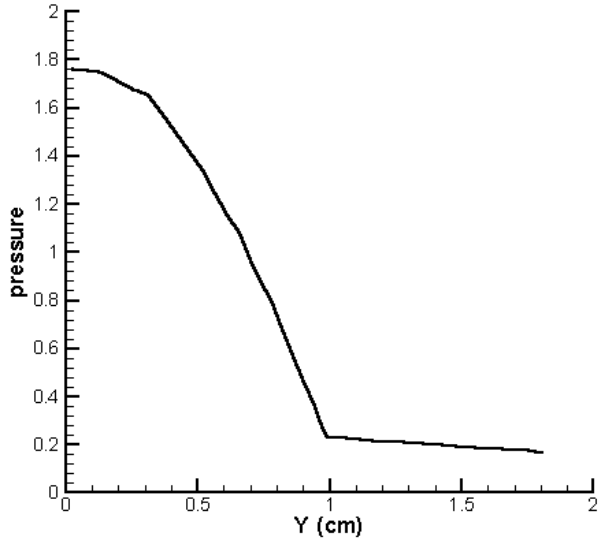

Figure 4. Pressure distribution along the surface, considering the viscous case (P / P_{∞}) .

The Figure 5 show the pressure contours obtained with freestream Mach number 9, pressure of 0.1847 atm and temperature of 300 K. The simulations considering inert gas flow. This result was obtained by using an axyssimetric formulation. The mesh used in this case has 9292 nodes and 17999 volumes.

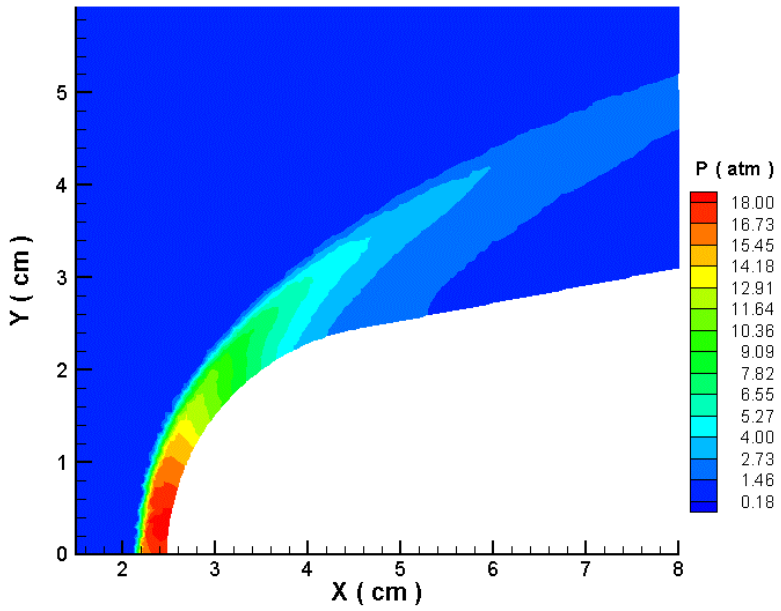

Figure 5. Pressure contours obtained with inert gas flow simulation.

One can observe that the pressure contours are well captured by this numerical method, the shock and the stagnation region are well represented. The pressure in the stagnation region reach maximum value of 18 atm. The streamline that passes through this normal portion of the shock impinges on the nose of the body and controls the values of stagnation pressure and temperature at the nose. The temperature contours are plotted in Figure 6.

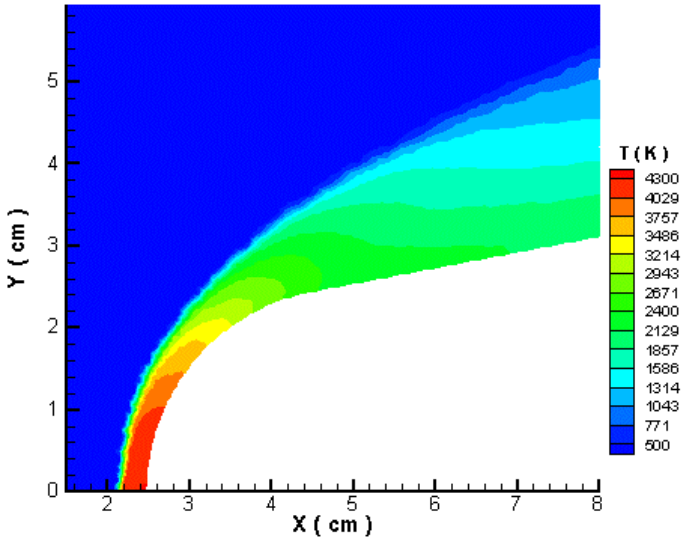

Figure 6. Temperature contours obtained with inert gas simulation.

The maximum temperature value in the stagnation region reaches 4300 K. If one considers real gas effects, the stagnation temperature would decay due the formation of species dissociation. The Figure 7 presents the pressure distribution along the surface, where the pressure is dimensionless.

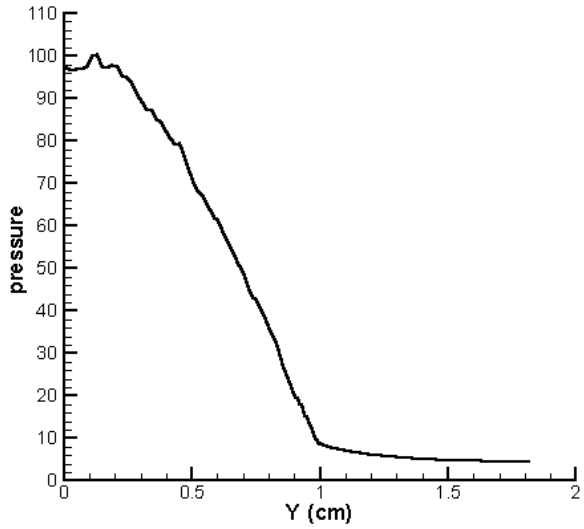

Figure 7. Pressure distribution over the surface (P / P_{∞}).

The oscillations presented in the pressure distribution indicate that more refined mesh must be used in the region near to the body's surface. The pressure decrease along the body, specially over a convex surface.

5. CONCLUSIONS

The present work performed an inviscid / viscous hypersonic flow simulations over a small ballistic re-entry vehicle SARA configuration. For the viscous case, the fluid was treated as a perfect gas. For the inviscid case, inert gas effects are incorporate into the solver. The governing equations are discretized in a cell centered finite volume algorithm. Unstructured meshes was used to obtain the numerical simulations. The equations are advanced in time by an explicit, 5-stage, 2^{nd}-order accurate, Runge-Kutta time stepping procedure. The spatial discretization scheme considered a 2^{nd}-order van Leer flux-vector splitting scheme. A MUSCL reconstruction of primitive variable extrapolation was performed in order to obtain left and right states at interfaces. The results indicated that the scheme was able to reproduce some phenomena presented in hypersonic flow.

6. ACKNOWLEDGMENTS

The first author thanks the support of CAPES (Coordenação de Aperfeiçoamento de Pessoal de Nível Superior) which allowed him to pursue graduate studies at Université de Poitiers (ENSMA et Faculte des Sciences Fondamentales et Appliques, France). The second author wishes to thank the Fundação de Amparo à Pesquisa do Estado de São Paulo (FAPESP, Brazil) for financial supporting. Also, the authors thanks the Agência Espacial Brasileira (AEB, Brazil).

7. REFERENCES

Anderson, Jr., J.D., "Hypersonic and High Temperature Gas Dynamics", McGraw-Hill, Inc., pp. 265-266, 1989.

Hirsh, C., Numerical Computation of Internal and External Flows. Vol. 2: Computational Methods for Inviscid and Viscous Flows, Wiley, New York, 1990.

Korzenowski, H., “Técnicas em Malhas não Estruturadas para Simulação de Escoamento a Altos Números de Mach” (Unstructured Grid Technique for Flow Simulation at High Mach numbers), doctoral Thesis, Instituto Tecnológico de Aeronáutica, June 1998, Brazil.

Mavriplis, D.J., “Multigrid solution of the two-dimensional Euler equation on Unstructured Triangular Meshes”, AIAA Journal, Vol. 26, No. 7, 1988, pp. 824-831.

Pimentel, C. A. R., Etude Numerique de La Transition entre Une Onde de Choc Oblique Stabilisee Par Un Diedre et Une Onde de Detonation Oblique, Thèse Doctorale, Université de Poitiers, 2000.

van Leer, B., “Flux-ecto Spliting for the Euler Equations,” Proceedings of the 8th International Conferenceon Numerical Methods in Fluid Dynamics, E. Krause, editor, Lecture Notes in Physics, vol. 170, 1995, pp. 507-512.